IRANIAN JOURNAL OF PHYSICS RESEARCH

Iranian Journal of Physics Research, Vol. 8, No. 2, 2008

Quantum transport in graphene normal-metal superconductor- normal-metal structures

H Mohammadpour and M Zareyan

Institute for Advanced Studies in Basic Sciences (IASBS), P. O. Box 45195-1159, Zanjan 45195, Iran

(Received 30 January 2008)

Abstract

We study the transport of electrons in a graphene NSN structure in which two normal regions are connected by a superconducting strip of thickness *d*. Within Dirac-Bogoliubov-de Gennes equations we describe the transmission through the contact in terms of different scattering processes consisting of quasiparticle cotunneling, local and crossed Andreev reflections. Compared to a fully normal structure we show that the angular dependence of the transmission probability is significantly modified by the presence of superconducting correlations. This modifation can be explained in terms of the interplay between Andreev reflection and Klein tunneling of chiral quasiparticles. We further analyze the energy dependence of the resulting differential conductance of the structure. The subgap differential conductance shows features of Andreev reflection and cotunelling processes, which tends to the values of an NS structure for large *d*s. Above the gap, the differential conductance shows an oscillatory behavior with energy even at very large *d*s.

Keywords: graphene, quantum transport, superconducting proximity, Klein tunneling, Andreev reflection

1. Introduction

Recently graphene a new material composed of carbon atoms arranged in two-dimensional honeycomb lattice which is a single atomic layer pulled out of bulk graphite, was synthesized by Geim's group in Manchester University [1]. Compared to the metallic and semiconducting materials, graphene has shown many intriguing electronic properties which have led to an explosion of studies in recent years [2, 3, 4, 5].

Due to its peculiar electronic band structure electrons in graphene behave like two dimensional mass less Dirac fermions [6]. In the hexagonal reciprocal space of graphene there are two non equivalent points K^+, K^-, the so called Dirac points, at the corners of the first Brillouin zone [7]. Around each of Dirac points, low energy electrons and holes have linear dispersion $\varepsilon(\vec{k}) = \pm\hbar v_F \left|\vec{k}\right|$, versus two-dimensional wave vector $\vec{k}$ with Fermi velocity $v_F \approx 10^6 m/s$ [7]. Thus the conduction (electrons) and valence (holes) conical bands touch at the points K^+, K^- ($\varepsilon(\vec{k}) = 0$) producing two nonequivalent valleys. This makes graphene a gapless semiconductor with relativistic-like dispersion of the excitations [8].

An electron in graphene structure is described by 4-component spinor $(\psi_A^+, \psi_B^+, \psi_A^-, \psi_B^-)$ in which, $\psi_{A(B)}^+$ is referred to the amplitude of the electron wave function on sublattice A(B) of the honeycomb structure with wave vector centered around the valley K^+; $\psi_{A(B)}^-$ are the corresponding wave functions for the valley K^- [6,8]. This spinor satisfies Dirac equation of the form [6,8]:

$$-i\hbar v_F \begin{pmatrix} H^+ & 0 \\ 0 & H^- \end{pmatrix} \psi = \varepsilon\psi, \qquad (1)$$

$$H^\pm = \sigma_x \partial_x \pm \sigma_y \partial_y,$$

where σ_x, σ_y are Pauli matrices describing pseudo spin space of two sublattices A and B.

Already anomalies of several quantum transport effects have been found in graphene. The integer QHE in graphene occurs with Hall conductivity plateaus appearing at half integer multiples of four (two spin and two valley degeneracy) times the quantum conductance e^2/h [2,3]. This quantization rule is caused by the quantum anomaly of the lowest Landau level in graphene which has a twice smaller degeneracy than the higher levels and its energy does not depend on the magnetic field [9].

Most of the studies are focused on the anomalies at

the limit of zero doping (zero charge carrier density) where the Fermi level is located close to the Dirac points. A finite conductance of order e^2/h is measured in graphene samples at Dirac point [10, 11, 12, 13]. This is surprising since one expects zero conductivity at this point where the electronic density of states vanishes.

The relativistic-like dynamics of electrons in graphene also affects the current fluctuations. Very recently the prediction of a finite shot noise in an undoped ballistic graphene was confirmed in the experiment [14]. For a wide ballistic graphene strip the Fano factor (the ratio of the noise power and the mean current) has the value $F = 1/3$ which corresponds to the shot noise power in a diffusive metallic contact [15, 16].

While graphene itself is not superconducting, but due to its atomic size thickness it can be superconducting by depositing a superconducting electrode on top of it [17]. Proximity induced Josephson effect between two superconducting graphene regions was predicted theoretically [18, 19, 20, 21] and observed in the experiment [22, 23]. Superconductivity in graphene can be described by Dirac-Bogoliubov-de Gennes (DBdG) equation [19] which takes into account electron-hole correlations, induced by the superconducting pair potential Δ. Within this equation it was found that a nonzero supercurrent can flow through a mesoscopic graphene sample even at the Dirac point with zero carrier concentration. Interestingly the Josephson current possesses a bipolar characteristic close to Dirac point where depending on the gate voltage the supercurrent carriers could be either the conduction band electrons or the valence band holes [18].

In Ref. [19] the superconducting proximity effect was studied in graphene NS contacts. As it is well known a special process called Andreev reflection (AR) [24] is responsible for the proximity effect in NS interfaces. AR is the conversion of an electron excitation into its time reversed hole when it hits the NS interface from N side with an energy lower than the superconducting energy gap Δ. AR in ordinary conductors is a retro reflection in which the electron and the reflected hole have opposite velocities [24]. In contrast it was found that in undoped graphene AR occurs in a *specular* manner where only the component perpendicular to the interface changes sign. This has a pronounced effect in the current-voltage characteristics of a graphene NS contact as explained in [19].

In addition to several quantum transport phenomena studied so far, there has been important studies of relativistic quantum electrodynamics phenomena in the context of graphene. The most famous effect is the reflection less tunneling of an electron from a potential barrier [25]. This is a condensed matter analog of the so called Klein paradox of relativistic quasi particles, that arises from the spinor nature of the wave functions in graphene and the relativistic linear spectrum [4]. This unique property of absence of back scattering could be regarded as responsible for extremely high mobility in graphene layers even at room temperature [2, 3]. The angular-dependence of the transmission probability through a potential barrier with perfect transmission at normal incidence has been explained theoretically [4].

In this paper we study a graphene NSN structure to see the interplay between AR taking place at the NS interfaces by the superconducting pair potential Δ and the Klein tunneling from the potential difference between S and N regions. Within scattering formalism and using DBdG equation in normal and superconducting regions we calculate the transmission amplitudes of electrons through the structure. The transmission processes contain different mechanisms which are electron cotunneling (CT), AR and crossed AR (CAR) [26, 27]. While AR occurs at an individual NS-interface, in CAR, incident electron and reflected hole emerge from different NS-interfaces.

Employing these transmission amplitudes in the Blonder-Tinkham-Klapwijk (BTK) formula [28], we have calculated the differential conductance of the structure. We analyze the energy-dependence of the differential conductance in different regimes corresponding to different values of the chemical potential in N and S regions compared to Δ and thickness of the S region d. We consider the limit of large mismatch between chemical potentials of S and N regions. We explain difference of angular-dependence of the transmission probabilities for low and high chemical potentials of the N regions where, respectively, specular and retro AR dominates the electron-hole conversion. Compared to the fully normal structure [4] we show that the angular-dependence of transmission is modified by the presence of the superconductivity.

The resulting differential conductance shows an oscillatory behavior at energies above Δ which persists even at thicknesses larger than the superconducting coherence length. At subgap energies, the behavior of the differential conductance is dominated by CAR and CT for thinner S region and by AR for thicker S region. We give a full analysis of differential conductance for different thicknesses of the S region and chemical potentials of the N regions.

2. Model and basic equations

We consider a graphene NSN structure occupying xy plane, as shown in Fig. 1. A wide superconducting strip (S) of thickness d connects two normal leads (N1 and N2). The normal leads are held at a voltage difference V and the voltage at S is zero. Using several electrostatic local gates, the chemical potential in different regions can be modulated. We consider the case where there is a chemical potential difference U between S and N regions. The potential profile then reads

$$U(\vec{r}) = \begin{cases} U, 0 < x < d \\ 0, otherwise \end{cases} \quad (2)$$

In the presence of superconducting correlations we use the DBdG equation which takes the form of two

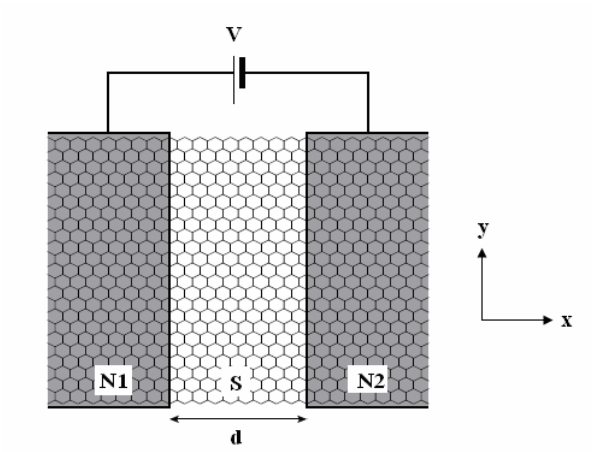

Figure 1. NSN structure on graphene

decoupled sets of equations as;

$$\begin{pmatrix} H^{\pm}+U(\vec{r})-E_F & \Delta \\ \Delta^{*} & E_F-U(\vec{r})-H^{\pm} \end{pmatrix}\begin{pmatrix} u \\ v \end{pmatrix}=\varepsilon\begin{pmatrix} u \\ v \end{pmatrix} \qquad (3)$$

with u and v being, respectively, two-component wave functions of electron-like and hole-like quasiparticles from two different valleys. Note that superconducting correlations couple an electron in one valley to its time-reversed hole in the other valley. E_F is the Fermi energy in normal leads and $\varepsilon > 0$ is the excitation energy measured from the chemical potential.

In N1 and N2 the pair potential $\Delta = 0$ and neglecting the suppression of superconductivity in S close to NS interfaces we take Δ to be real and constant inside S. This assumption is most valid when the Fermi wave length in region S is much smaller than the Fermi wave length in region N, namely when $U >> E_F$. Because of the valley degeneracy, we will consider only one set of the four-dimensional equations (3) which describes coupling of electrons from valley K^{+} to holes from valley K^{-}.

Due to the one dimensional nature of the applied potential, the wave vector in the direction parallel to the boundaries (q) is constant in the three regions.

Assuming an incident electron with probability amplitude 1 from N1, the solution of Eq. (3) inside N1, S and N2 are, respectively, written as the followings

$$\begin{aligned} \psi_{N1} &= \psi^{+}_{Ne} + r\psi^{-}_{Ne} + r_A\psi^{-}_{Nh}, \\ \psi_{S} &= a\psi^{+}_{Se} + b\psi^{-}_{Se} + c\psi^{+}_{Sh} + d\psi^{-}_{Sh}, \\ \psi_{N2} &= t_e\psi^{+}_{Ne} + t_h\psi^{+}_{Nh}, \end{aligned} \qquad (4)$$

where $\psi^{\pm}_{Se,Sh}$ are bases of DBdG in S which describe electron-like (e) and hole-like (h) quasiparicles which propagate in $\pm$ directions of x axis. Correspondingly in N1 and N2, $\psi^{\pm}_{Ne,Nh}$ are the electron and hole bases propagating in $\pm x$ directions. The bases are given by

$$\begin{aligned} \psi^{\pm}_{Se} &= \exp(iqy \pm ik_0x \mp kx)\begin{pmatrix} \exp(i\beta) \\ \pm\exp(\pm i\gamma + i\beta) \\ 1 \\ \pm\exp(i\gamma) \end{pmatrix}, \\ \psi^{\pm}_{Sh} &= \exp(\pm iqy \mp ik_0x \mp kx)\begin{pmatrix} \exp(-i\beta) \\ \mp\exp(\mp i\gamma - i\beta) \\ 1 \\ \mp\exp(-i\gamma) \end{pmatrix}, \end{aligned} \qquad (5)$$

$$\begin{aligned} \psi^{\pm}_{Ne} &= \frac{\exp(iqy \pm ik_ex)}{\sqrt{\cos\alpha}}\begin{pmatrix} \exp(\mp i\alpha/2) \\ \pm\exp(\pm i\alpha/2) \\ 0 \\ 0 \end{pmatrix}, \\ \psi^{\pm}_{Nh} &= \frac{\exp(iqy \pm ik_hx)}{\sqrt{\cos\alpha'}}\begin{pmatrix} 0 \\ 0 \\ \exp(\mp i\alpha'/2) \\ \mp\exp(\pm i\alpha'/2) \end{pmatrix}, \end{aligned} \qquad (6)$$

where

$$\beta = \begin{cases} \arccos(\frac{\varepsilon}{\Delta}), & if\ \varepsilon < \Delta \\ -i\,\mathrm{arccos}\,h(\frac{\varepsilon}{\Delta}), & if\ \varepsilon > \Delta \end{cases},$$

$$\gamma = \pi + \arcsin(\hbar v_F q / |E_F - U|),$$

$$k_0 = \sqrt{(E_F-U)^2/(\hbar v_F)^2 - q^2}\ ,$$

$$k = \frac{(E_F-U)\Delta}{(\hbar v_F)^2 k_0}\sin\beta$$

and

$$\begin{aligned} k_e &= (\hbar v_F)^{-1}(\varepsilon + E_F)\cos\alpha, \\ k_h &= (\hbar v_F)^{-1}(\varepsilon - E_F)\cos\alpha' \end{aligned} \qquad (7)$$

Here $\alpha = \arcsin(\hbar v_F q/(\varepsilon + E_F)) \in [-\pi/2, \pi/2]$ and $\alpha' = \arcsin(\hbar v_F q/(\varepsilon - E_F))$ are, respectively, the angles that an electron and hole wave vectors make with x axes. We note that beyond a critical angle of incidence defined by

$$\alpha_c = \arcsin(|\varepsilon - E_F|/(\varepsilon + E_F)), \qquad (8)$$

α' becomes imaginary and so there is no AR and CAR. The coefficients a, b, c and d are relative amplitudes of different wave functions in S. r and r_A are, respectively, amplitudes of electron normal and Andreev reflections in N1. For an incident electron in N1 , t_e and t_h are the amplitudes of transmission of an electron and hole into N2 which describe CT and CAR processes respectively. Note that while in N1 and N2 the wave functions are propagating for all ε , in S they are propagating only for

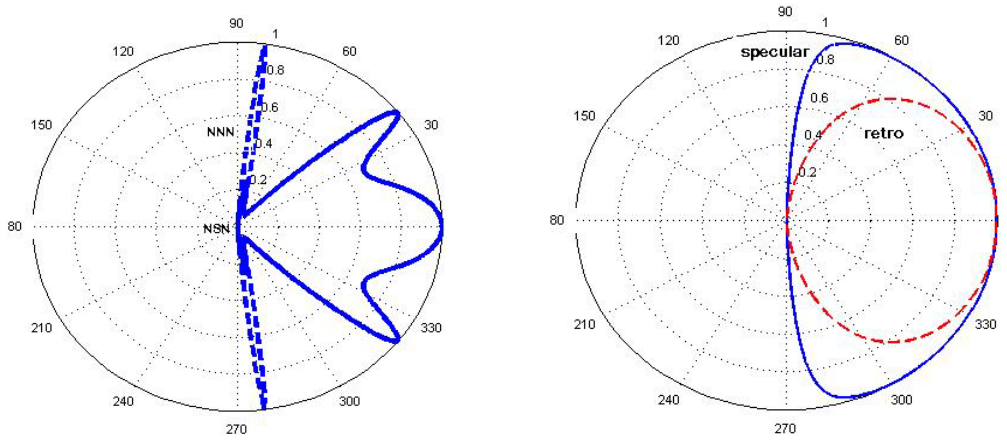

(a) (b)

Figure 2. $T(\alpha)$ in NSN structures with $d/\xi = 0.122$, $\varepsilon/\Delta = 0$ and (a) $U/\Delta = 243, \Delta/E_F = 0$ (dashed curve), $\Delta/E_F = 0.01$ (solid curve), (b) specular and retro reflection regimes by $\Delta/E_F = 20,\ 0.01, U/\Delta = 10^9$.

$\varepsilon > \Delta$. For $\varepsilon < \Delta$ the wave functions are evanescent inside S where they have an exponential decay along x direction within a scale of order $\xi = \hbar v_F / \Delta$.

In contrast to the parabolic energy spectrum in ordinary two dimensional electron gas (2DEG) which requires the continuity of the derivatives of the wave functions as well as their amplitudes, for chiral electrons in graphene the velocity is constant irrespective of the energy; so, one has to impose only the continuity of the wave functions for each sublattices which also conserves the chirality. Imposing the continuity condition at N1S and SN2 interfaces we have the relations

$$\psi^{+}_{Ne} + r\psi^{-}_{Ne} + r_A\psi^{-}_{Nh} = a\psi^{+}_{Se} + b\psi^{-}_{Se} + c\psi^{+}_{Sh} + d\psi^{-}_{Sh} \quad (9)$$

at $x = 0$ and

$$a\psi^{+}_{Se} + b\psi^{-}_{Se} + c\psi^{+}_{Sh} + d\psi^{-}_{Sh} = t_e\psi^{+}_{Ne} + t_h\psi^{+}_{Nh} \quad (10)$$

at $x = d$. These relations constitute a system of 8 linear equations whose solutions give us r, r_A, t_e and t_h. The relation $|r|^2 + |r_A|^2 + |t_e|^2 + |t_h|^2 = 1$ holds for ensuring current conservation.

The differential conductance of the system, $\partial I/\partial V$ for $\varepsilon = e \times V$ is calculated by the BTK formula as:

$$\frac{\partial I}{\partial V} = g_0(V)\int_0^{\alpha_c} (1 - |r(eV,\alpha)|^2 + |r_A(eV,\alpha)|^2)\cos\alpha\, d\alpha$$
$$g_0(V) = 4e^2/h \times N(eV),$$
$$N(\varepsilon) = (E_F + \varepsilon)W/\pi\hbar v_F \quad (11)$$

where g_0 is the conductance of N transverse modes in a ballistic graphene strip of width W. In our model we consider a wide geometry of $W >> d$ for that $N >> 1$.

3. Results and discussion

First we analyze the angular dependence of the transmission probability $T(\alpha) = 1 - |r(\alpha)|^2$ for electrons. We note that for $\varepsilon << E_F$, in contrast to the amplitude of AR, amplitude of CAR is small since it requires a change of pseudospin.

In Fig. 2a we have plotted $T(\alpha)$ at the Fermi level $\varepsilon = 0$ when $U/\Delta = 243$ for both superconducting ($\Delta/E_F = 0.01$) and normal strip ($\Delta = 0$) cases. In the normal case there is always a perfect transmission at normal incident $\alpha = 0$ due to Klein tunneling [4]. Additional perfect transmissions can occur at larger angles due to the resonances which for given U and d are defined by the solutions of the following equation

$$4\sin^2\gamma\sin^2 kd + \sin 2\gamma \sin 2kd$$
$$-2\sin\alpha\cos\gamma\sin 2kd - \quad (12)$$
$$4\sin\alpha\sin\gamma\sin^2 kd = 0$$

Introducing superconductivity leaves the transmission probability intact at almost normal incidence, but suppresses the transmission at larger angles. In the case of Fig. 2a the resonance at $\alpha \approx \pi/2$ disappears by superconductivity. We can understand this behavior by noting that a retro AR conserves the pseudospin and thereby the reflection-less tunneling through S is preserved at small angles. However the resonant transmission at larger angles is affected by evanescent nature of the subgap quasiparticles in S strip leading to a suppression of transmission probability.

Fig. 2b represents an example of comparison of $T(\alpha)$ in two limits of retro ($\Delta/E_F = 0.01$) and specular ($\Delta/E_F = 20$) AR regimes for $U/\Delta = 10^9$, $\varepsilon/\Delta = 0$, $d/\xi = 0.122$. This shows a remarkable difference in the angular dependence in two cases which

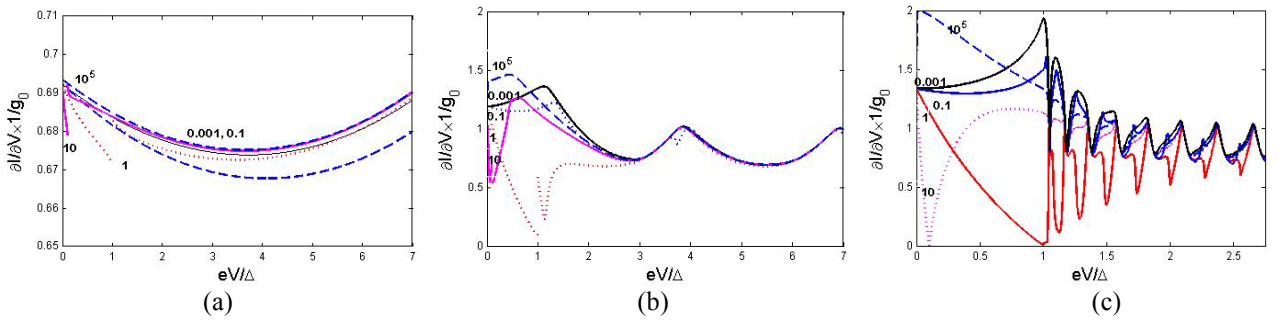

Figure 3. $g_0^{-1}\partial I/\partial V$ in different regimes for $U/\Delta = 10^9$, for $d/\xi =$ (a) 0.1, (b)1, (c) 10; scales are different to reveal the d -dependent period of the oscillation. The values of Δ/E_F are written beside each plot.

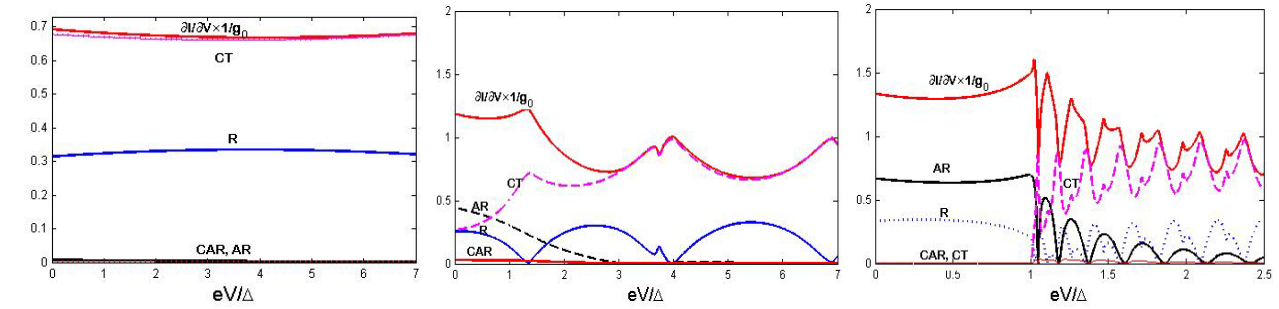

Figure 4. Separate contribution of each propagation probability in $g_0^{-1}\partial I/\partial V$, with $\Delta/E_F = 0.1$ for $d/\xi =$ (a) 0.1, (b) 1, (c) 10 when $U/\Delta = 10^9$.

depends on d and U .

Now let us analyze the behavior of the differential conductance, $\partial I/\partial V$ which is given by Eq. (11). Fig. 3 shows $g_0^{-1}\partial I/\partial V$ versus eV/Δ when $U/\Delta = 10^9$ for thicknesses, $d/\xi = 0.1, 1, 10$ and for different Δ/E_F to cover whole range from pure specular to pure retro AR.

For a thin strip with $d/\xi = 0.1$ (Fig. 3a) the transport is dominated by CT which results in a normalized differential conductance $g_0^{-1}\partial I/\partial V$ close to unity. The subgap differential conductance shows small deviations due to weak AR amplitude. Above the gap, by increasing the voltage, $g_0^{-1}\partial I/\partial V$ increases to unity in an oscillatory manner. The period of oscillations is inversely proportional to the thickness.

Increasing the thickness of S strip leads to an increase in the amplitude of AR and thus enhancing deviations from normal differential conductance at subgap voltages. This is seen in Fig. 3b where $g_0^{-1}\partial I/\partial V$ is plotted for $d/\xi = 1$. Above the gap $g_0^{-1}\partial I/\partial V$ shows quantum interference oscillations with smaller period compared to $d/\xi = 0.1$. Note that the period of oscillations does not depend on the doping of N regions given by Δ/E_F . In contrast to this, below the gap, behavior of $g_0^{-1}\partial I/\partial V$ strongly depends on Δ/E_F . This can be understood by noting that contributions of two different types of retro and specular ARs in electron transmission depend on Δ/E_F . The Andreev transmission ranges from purely retro reflection at $\Delta/E_F << 1$ to purely specular reflection at $\Delta/E_F >> 1$ [19].

By further increasing d/ξ , the contribution of CT becomes even smaller at subgap voltages. The subgap differential conductance is determined only by AR. As a result, $g_0^{-1}\partial I/\partial V$ takes zero value at $eV = E_F$ (Fig. 3c) for that the AR is forbidden since the critical angle $\alpha_c = 0$ (Eq.(8)). Therefore the subgap conductance of very large d/ξ is very similar to that of NS system [19]. Above the gap, $g_0^{-1}\partial I/\partial V$ is oscillating with energy as two previous cases. The oscillations persist even at very large thicknesses due to the ballistic feature of the contact.

To give more insight into different scattering processes, in Fig. 4 we have plotted contributions of CT, AR, CAR and R to differential conductance for different thicknesse and for $\Delta/E_F = 0.1$. These plots confirm the above given explanations. Note that the contribution of CAR is always small because in contrast to AR, CAR requires a change of pseudospin which is prevented in the absence of psudospin flip scattering.

4. Conclusions

In this paper we have studied quantum transport of electrons through a graphene superconducting strip which connects two normal leads. Using DBdG equations we have calculated amplitudes of different scattering

processes which are normal reflection, direct and crossed Andreev reflections and cotunneling. First we have observed superconducting induced changes in the angular dependence of the electron transmission which can be explained in terms of interplay between Klein tunneling, Andreev reflection and resonance transmission. Within BTK formalism we have analyzed the resulting differential conductance for different thicknesses of the S strip and doping degrees of the N electrodes. The subgap $eV/\Delta < 1$ differential conductance is determined by the competition of Andreev reflection and cotunneling. While in the limits of $d/\xi << 1$ and $d/\xi >> 1$ the transmission is respectively, dominated by purely cotunneling and Andreev reflection processes, at intermediate thicknesses $d/\xi \approx 1$, it is determined by superposition of both processes. Above the gap $eV/\Delta > 1$, the differential conductance shows oscillatory behavior with eV/Δ. We have given a full analysis of the period and the amplitude of this quantum interference oscillations in terms of d/ξ and doping of N regions.

References

1. K S Novoselov et al., *Science*, **306** (2004) 666.
2. K S Novoselov, A K Geim, S V Morozov, D Jiang, M I Katsnelson, I V Grigorieva, S V Dubonos, and A A Firsov, *Nature* **438** (2005) 197.
3. Y Zhang, Y-W Tan, H L Stormer, and P Kim, *Nature* **438** (2005) 201.
4. M I Katsnelson, K S Novoselov, and A K Geim, *Nat. Phys*. **2** (2006) 620.
5. K Nomura and A H MacDonald, *Phys. Rev. Lett*. **98** (2007) 76602.
6. D DiVincenzo and E Mele, *Phys. Rev.* B **29** (1984) 1685.
7. K S Novoselov, et al., *Nature* 438 (2005) 197; Y Zhang, et al., *Nature* **438** (2005) 201.
8. P R Wallace, *Phys. Rev*. **71** (1947) 622.
9. V P Gusynin, V A Miransky, and I A Shovkovy, *Phys. Rev. Lett*. **73** (1994) 3499; *Phys. Rev*. D **52** (1995) 4718.
10. A W W Ludwig, M P A Fisher, R Shankar, and G Grinstein, *Phys. Rev.* B 50 (1994) 7526.
11. K Ziegler, *Phys. Rev. Lett*. **80** (1998) 3113.
12. N M R Peres, F Guinea, A H Castro Neto, *Phys. Rev.* B **73** (2006) 125411.
13. K Nomura and A H MacDonald, *Phys. Rev. Lett*. **95** (2006) 256602; I L Aleiner and K B Efetov, *Phys. Rev. Lett*. 91 (2006) 366801; A Altland, *Phys. Rev. Lett*. **97** (2006) 236802.
14. J Tworzydlo, B Trauzettel, M Titov, A Rycerz, and C W J Beenakker, *Phys. Rev. Lett*. **96** (2006) 246802.
15. C W J Beenakker and M B¨uttiker, *Phys. Rev*. B **46** (1992) 1889.
16. K E Nagaev, *Phys. Lett*. A **169** (1992) 103.
17. A F Volkov, P H C Magnee, B J van Wees, and T M Klapwijk, *Physica* C **242** (1995) 261.
18. M Titov and C W J Beenakker, *Phys. Rev*. B **74** 041401(R) (2006).
19. C W J Beenakker, *Phys. Rev. Lett.* **97** (2006) 067007.
20. A G Moghaddam, M Zareyan, *Phys. Rev. B* **74** 241403(R) (2006).
21. A G Moghaddam, M Zareyan, *Appl. Phys. A* **89** (2007) 579.
22. H B Heersche, P Jarillo-Herrero, J B Oostinga, L M K Vandersypen, A F Morpurgo, *Nature* **446** (2007) 56.
23. A Shailos, W Nativel, A Kasumov, C Collet, M Ferrier, S Gueron, R Deblock, H Bouchiat, *Euro. Phys. Lett*. **79** (2007) 57008.
24. A F Andreev, Zh Eksp. *Teor. Fiz*. **46** (1964) 1823; Sov. Phys. JETP **19** (1964) 1228.
25. O Klein, *Z Phys.* 53 (1927) 157.
26. J M Byers and M E Flatté, *Phys. Rev. Lett*. **74** (1995) 306.
27. G Deutscher and D Feinberg, *Appl. Phys. Lett*. **76** (2000) 487.
28. G E Blonder, M Tinkham, and T M Klapwijk, *Phys. Rev.* B **25** (1982) 4515.